Evaluation of Flying Caching Servers in {UAV}-{BS} based realistic environment

Evaluation of Flying Caching Servers in UAV-BS based realistic environment

German Castellanos[a,c,*], Greta Vallero[b], Margot Deruyck[a], Luc Martens[a], Michela Meo[b] and Wout Joseph[a]

[a]Department of Information Technology, IMEC-Ghent University, 9052 Ghent, Belgium.
[b]Department of Electronics and Telecommunications (DET), Polytechnic University of Turin, 10129 Turin,Italy
[c]Department of Electronics Engineering, Colombian School of Engineering, 111166, Bogota Colombia.

ARTICLE INFO

Keywords:
UAV-BS
Flying Caching Servers
Unmanned aerial vehicle networks
Multi-Access Edge Caching
Backhaul
Radio Access Network.

ABSTRACT

The dramatic growth of data traffic during the past decade has challenged wireless networks to provide new mechanisms to support such demand. Fast deployable wireless networks supported by Unmanned Aerial Vehicles (UAV) are a promising solution, especially to support in crowded scenarios with high peaks of traffic. Nevertheless, mounting a Base Station (BS) on UAVs (UAV-BSs) raises several challenges like the saturation of the backhaul (BH) link, needed for the communication between them and the Core Network (CN). In this work, this issue is addressed with the usage of the Multi-Access Edge Computing (MEC) technology, consisting on the placement of servers, providing computing platforms and storage, directly at the edge of these networks, e.g. on the UAV-BSs. In particular, we consider a portion of a Radio Access Network (RAN) composed by UAV-BSs, equipped with servers that provide the caching capability. The performance is evaluated, using realistic traffic demand, for different traffic characteristics, capacity of the cache server and users' density. Simulation results reveal that the usage of the MEC caching prevents the BH network saturation, since in case a requested content is locally cached, the BH network is not used. As consequences, the user coverage and the access capacity increase up to 33% and 70%, respectively and the experienced delay drops by 30%.

1. Introduction

In recent years, wireless network traffic has been increasing rapidly. Indeed, a 23 times growth in the global mobile data traffic is expected in 2021, compared to the entire global Internet traffic in 2005 [1]. According to International Telecommunication Union (ITU), the overall mobile data traffic will grow with an exponential trend until 2030, reaching five zettabytes (ZB) per month. To face this trend, fast deployable and dynamic wireless networks are needed [2, 3]. For the implementation of these networks, mounting a BS on an UAV, commonly known as drone, represents a promising solution. A BS is attached to an UAV, which flies where needed and provides radio access capacity in the covered area. In order to connect that BS to the Core Network (CN), Backhaul (BH) links are established. In 5G networks, the UAV access networks have been considered for scenarios like festivals, concerts, sports matches and natural disasters, when the terrestrial network fails due to congestion or physical unavailability. The usage of drones as Unmanned Aerial Vehicle - Base Stations (UAV-BS) brings connectivity to the users that are suffering from low-quality of service [4, 5, 6, 7]. According to [1], also in the next 6G networks, the drone cells or UAV wireless networks will be the key to achieve cell-free networks, acting as flying BSs to provide radio coverage. Moreover, these UAV-BSs will be also used as content providers and computing servers, employing the Multi-Access Edge Computing (MEC) technology, previously known as Mobile Edge Computing technology. This technology pushes storage and computational capabilities at the edge of the network closer to users, in order to reduce the latency and the load in the CN, since it makes unneeded the access in the core network [1, 8, 9, 10, 11, 12].

In order to totally exploit the potential of the UAV-BS networks, several challenges need to be addressed, such as the proper location of the UAV-BSs and the optimisation of the radio resource allocation to cope with the limit imposed by the access, and the BH network capacity [1, 13, 14, 15, 16]. In the literature, effort has been put in the design of UAV-BSs Radio Access Network (RAN). Nevertheless, the BH network has been investigated just recently.

According to our previous work presented in [17], the BH network is the most challenging part of this network. Indeed, its links represent the bottleneck of the system. Working in the 3.5 GHz band, with or without Carrier Aggregation (CA), the user coverage is not larger than 74% because of the capacity constraints of the BH links. While using the 60 GHz band instead, the BH capacity increases since more bandwidth is available in this area of the spectrum. Nevertheless, the user coverage does not reach values larger than 68%, since the high path loss makes the radius coverage shorter. In this paper, to address this issue, we propose the usage of the MEC technology, to push computing and storage platforms on servers at the edge of the network.

*Corresponding author
german.castellanos@ugent.be (German Castellanos); greta.vallero@polito.it (Greta Vallero); Margot.Deruyck@UGent.be (Margot Deruyck); Luc1.Martens@UGent.be (Luc Martens); michela.meo@polito.it (Michela Meo); Wout.Joseph@UGent.be (Wout Joseph)
ORCID(s): 0000-0001-7511-2910 (German Castellanos); 0000-0002-6420-231X (Greta Vallero); 0000-0001-9948-9157 (Luc Martens); 0000-0001-7403-6266 (Michela Meo); 0000-0002-8807-0673 (Wout Joseph)

In this work, we consider a crowded scenario of a soccer stadium, where the RAN is given by a set of UAV-BSs, equipped with MEC servers, which store popular contents. This scenario is simulated with a realistic 3D model of the city centre of Ghent, in Belgium, used in our previous works presented in [5, 17, 18, 19].The novelties of this research are the following:

- A MEC - UAV-BS based network architecture with simultaneous allocation of resources in the access and BH links considering the caching capabilities of the MEC servers and the constrains of the wireless LTE technology used.
- A capacity and coverage study in a 3D modelled city while considering a realistic dynamic data traffic in an overcrowded scenario.
- A power consumption evaluation of the MEC - UAV-BS architecture during a crowded event.

To the best of the authors' knowledge, similar evaluations have not been done yet.

The paper is organised as follows. Section 2 describes related works reviewing the usage of UAV in wireless communications, the MEC technology and its caching feature and recent advances in flying caching servers. Section 3 presents a systematic model and defines the subscribed problem, including the network, MEC server, power consumption, time delay, traffic demand and channel modelling. Section 4 provides an overview of the scenario used, introduces the network architecture used and the tool developed to solve the proposed problem, while the key performance indicators are presented in Section 5. Section 6 discusses the results and finally, Section 7 draws the conclusions and future work.

2. Flying Caching Servers

This section portrays the recent advances in the UAV-BS networks and the caching server technologies, and presents an insightful review of the MEC technologies deployed for UAV-BS found in the literature.

2.1. UAV-BS Networks

Recently, studies about the concept of using BSs mounted in drones or UAV, have been published [4, 20, 21, 22, 23, 24, 25, 26]. Mozaffari et al. in [4] introduce an extensive tutorial about wireless networks aided by UAV. In this work, the classification of a wireless network with UAVs, the open issues related to the channel modelling, the optimal trajectory and deployment, the network planning, and the resource management are presented. Authors in [20, 21, 22] provide diverse overviews that cover different aspects of the UAV-aided networks, starting from the fundamentals of aerial channel modelling to specific performance indicators to evaluate aerial wireless networks. The survey in [23] focuses on the challenges of the physical aspects of multi-UAV networks such as the flight control and trajectory planning and cross-layer network design for mission control applications. The reference [24] presents the characterisation of UAV-BSs based networks, their architectures and the problematic of data routing, handovers and the impact of energy efficiency. In [25], the concept of 3D aerial networks is presented and all its challenges are discussed. Alzahrani et al. [26] present a comparative study of UAV-aided networks and point out numerous challenges.

The study of the backhaul impact on UAV-aided networks is relatively recent. In [27] a multi-hop BH network is proposed to maximise the bitrate of the UAV-BS nodes through a network formation game algorithm. Gapeyencho et al. [28] provide a BH network for UAV-BS based in mm-Wave 3GPP standards, evaluating the impact of moving 3D objects on the propagation links of mm-waves. [17] and [29] propose similar evaluations to Long Term Evolution (LTE) based BH link for UAV-BS. The authors agree that the increment of the ground nodes density leads to a diminish in the BH quality due to the saturation of the resource block (RB) usage. Similarly, in [30] an optimal solution for an LTE in-band integrated access and BH network is evaluated for a single drone where the usage of UAV-BS enhances throughput. Unfortunately, in this study, only a few User Equipment (UEs) are considered; thus, saturation of the channel is not achieved. In a more practical approach, Pokorny et al. [31] present a prototype of an mm-Wave antenna steering for the BH link that provides connectivity to aerial BS. Likewise, in [32] simulations and measured camping results are provided to explore realistic access and BH links further, where the flight time, BH link distance and mm-Wave alignments were the mayor limitations found. Additional studies of resources allocation and UAV-BS's 3D trajectory and placement where BH constraints are solved using optimisation methods [33, 34, 35, 36] could be found in the literature.

2.2. Multi-Access Edge Computing

The MEC technology, that uses computing and caching power at the edges of the network, has received much attention in the literature, since it provides several benefits, such as the reduction of the experienced latency and of the load in the core network, since storage and computational capabilities are pushed next to end-users [11, 37]. The reduction of the latency given by the adoption of the MEC paradigm in wireless networks is demonstrated in [8, 38]. In [8], different use cases show the impact given by the usage of the MEC paradigm, when providing collaborative video caching and multi-layer interference cancellation. The work presented in [38] highlights that the spectral and energy efficiency are improved with caching at the wireless edges. Many works formulate an optimisation problem to select the contents to cache in order to improve the network performance, when the MEC technology is used [9, 10, 39, 40, 41, 42].

Authors in [9] aim at minimising the experienced delay in an heterogeneous RAN, where caching servers are placed on each BS. In [10], the optimisation problem maximises the local hit, proposing a reduction of the problem in order to treat it analytically. With the same objective, in [11], the

optimal content placement problem is given. The work discussed in [40] formulates through an integer programming problem the proper content placement in order to optimise the system towards the hit occurrences and the power consumption, considering users mobility. Also in [41], the experienced delay and power consumption are jointly optimised and results are obtained through simulations. In [42], the allocation of femtocells and WiFi off-loading, used as helper where some contents are cached, is optimised aiming to minimise the time needed for each download.

2.3. MEC in the Air

The UAV-aided networks coupled with MEC capacities are explored in [43]. They describe a two-tier heterogeneous network architecture and discuses the open issues of MEC in the context of UAV-aided networks. In [44], Chen et al. introduce the concept of caching in the sky and present an optimisation problem between the relation users and UAV-BS, the location of the UAV and the cache contents of each UAV. Here, the goal is to maximise the Quality-of-Experience (QoE) of each user while minimising the transmitted power, aided by Echo State Network (ESN) based Machine Learning (ML) algorithms. Likewise, the authors of [45] focus on the optimal UAV-BS placement maximising the achievable bitrate of the access network through a decode-and-forward caching system.

In [46], an UAV-BS network is deployed with caching capabilities in peak hours to alleviate small ground BSs; to guarantee the security of the network, jamming signals from the small idle BSs are introduced. Power control in ultra-dense networks supported by UAV is described in [47], where caching, energy transfer and relaying capabilities are evaluated. The authors of [48], present a joint optimisation problem aiming to maximise the throughput of IoT devices using multimedia traffic. The 3D location of the UAVs is evaluated through enumeration search method. Furthermore, the probability of placing a caching server on specific UAV is calculated too. The authors of [49] propose a scheme to reduce the cost of the information platform employing a bidding strategy for the tasks published by the platform which ultimately will determinate the optimal trajectory of the UAVs. Contradictory of the network-centric approaches described so far, the authors of [50] propose a proactive caching service where files are cached in users after being proactive delivered by UAV. This problem is evaluated by maximisation file caching and file retrieval cost functions.

Further studies of the location and placement of UAV-BS with caching capabilities are explored in [51, 52, 46]. In [53] and [54], Internet of Things (IoT) networks are considered. In this scenario, because of the limited local computing capabilities of sensors, the usage of UAVs as edge computing servers is very promising, in order to offload some tasks. Finally, some Machine Learning (ML) algorithms to solve the placement of UAV-BS under caching server scenarios are collected in [55, 56, 57, 58].

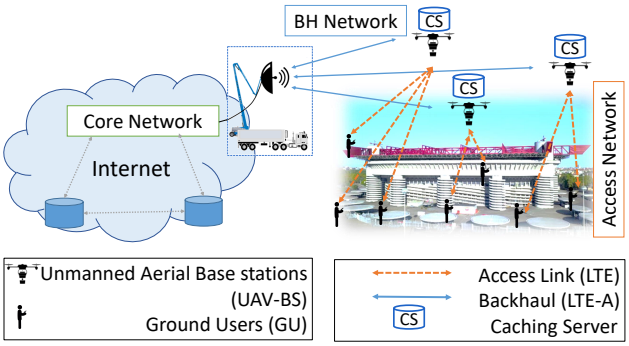

Figure 1: Architecture of Flying Caching Servers

3. System Model

We consider an UAV-BS aided network to support a crowded scenario, like a soccer match or a festival, depicted in Fig.1. The following subsections describe in detail this system model. First we describe the models for the network and the MEC server. Then we outline the power consumption, time delay and traffic demand used in our system and finalise with the channel models. Details of the notations of these models could be found in Tables 1, 2 and 3.

3.1. Network Modelling

In order to model the architecture depicted in Fig.1, a fleet of N UAV-BSs, acting as traditional BSs is used. These N UAV-BSs provide the communication service to the U ground users. Each ground user u access this service through the access network (orange links in Fig.1), provided by the N UAV-BSs. These UAV-BSs reach the CN through BH links (blue links in Fig.1). We assume that time is slotted in T time slots. Each UAV-BS $n \in [1, N]$ has a certain access capacity, i.e., it can deliver up to $B_a \geq 0$ data volume, in bits, within each time period t in the access network. Similarly, $B_{BH} \geq 0$ is the maximum traffic volume which can be carried in the BH network, within each time slot t. This means that, given $b_{a,n}^{(t)}$ and $b_{BH,n}^{(t)}$ the traffic volume carried by each UAV-BS n in the access and BH network at time t, respectively, the following conditions have to be satisfied:

$$b_{a,n}^{(t)} \leq B_a \qquad \forall n \in [1, N], B_a \geq 0, b_{a,n} \geq 0 \tag{1}$$

$$\sum_{n=1}^{N} b_{BH,n}^{(t)} \leq B_{BH} \qquad B_{BH} \geq 0, b_{BH,n} \geq 0 \tag{2}$$

3.2. MEC Server Modelling

We assume that each UAV-BS n is equipped with a MEC server, that provides the caching capability. The server of each UAB-BS n updates its cached contents according to the Least Frequently Used (LFU) cache algorithm, to store the C most popular contents. We assume a library $\mathcal{F}=\{1, 2, .., F\}$, composed by F content items. Each file has size S, in bits,

Table 1
Summary of the system model notation.

Notation	Definition
N	Number of UAV-BS in the fleet
U	Number of users
T	Number of time slots
C	Maximum number of cached contents
B_a	Maximum access capacity of each UAV-BS
B_{BH}	Maximum BH network capacity
$b_{a,n}^{(t)}$	Traffic volume carried by UAV-BS n in the access network
$b_{BH,n}^{(t)}$	Traffic volume carried by UAV-BS n in the BH network
$\mathcal{F}$	Set of contents in the library
F	Number of contents in the library
S	Size of each content
$P_{\mathcal{F},n}(f)$	PDF of the content popularity of UAV-BS n
α	Parameter of the Zipf's distribution
p_{hit}	Hit probability
p_{miss}	Miss probability
$l_u^{(t)}$	Traffic volume requested by user u at time t
$P(t)$	The network power consumption at time t
$P_{a,n}^{(t)}$	The access power consumption of UAV-BS n, at time t
$P_{BH,n}^{(t)}$	The BH power consumption of UAV-BS n, at time t
$P_{c,n}^{(t)}$	The caching power consumption of UAV-BS n, at time t
D	Average transmission delay
D_{hit}	Time needed to send a content from an UAV-BS to a user
D_{miss}	Time needed to send a content from the cloud to a user

and this assumption can be easily removed, since in real systems, files can be split into blocks of the same length [59, 60]. Moreover, each file has its popularity, which varies geographically, i.e., each UAB-BS n is characterised by a specific order of popularity of contents, described with a Probability Density Function (PDF) $P_{\mathcal{F},n}(f)$. As consequence, it is possible that the probability that the content f is required on UAV-BS ϕ is different than on UAV-BS θ, with $\phi \neq \theta$. Nevertheless, for each UAV-BS $n, n \in [1, N]$, $\sum_{f=1}^{F} P_{\mathcal{F},n}(f) = 1$. As in [40, 9, 41, 61, 42], the popularity is described by a Zipf's distribution, which is expressed as:

$$P_{\mathcal{F},n}(f) = \frac{\Omega}{f^{\alpha}} \tag{3}$$

where $\Omega = (\sum_{i=1}^{F} \frac{1}{i^{\alpha}})^{-1}$ [41]. The parameter α impacts the difference among contents in terms of popularity and defines the steepness of the Zipf's distribution. A large value of α (i.e., $\alpha > 1$) means that the most popular contents are significantly more popular than the other contents. By decreasing α, the popularity of content behaves more similarly to a uniform distribution. As in [41], since the local most popular contents are stored in the server of each UAV-BS n, the hit probability is as follows:

$$p_{hit} = 1 - \frac{\sum_{f=C}^{F} \frac{1}{f^{\alpha}}}{\sum_{f=1}^{F} \frac{1}{f^{\alpha}}} \tag{4}$$

where, as previously mentioned, C is the number of contents stored in each cache, F is the number of items in the library. As can be noticed in (4), p_{hit} is monotonic increasing with C. The miss probability p_{miss} is computed as $p_{miss} = 1 - p_{hit}$, resulting in monotonic decrease with C. We denote by $l_u^{(t)}$ the traffic volume which is associated to the user u, $u \in [1, U]$, at time t and we model the number of contents, which each user u requires, as $\lfloor \frac{l_u^{(t)}}{S} \rfloor$, where the $\lfloor \cdot \rfloor$ operator is needed to represent an integer number of requests for content per user. We denote by $\mathcal{U}_n^{(t)}$ the set of users who are associated with UAV-BS n, at time t. This means that $b_{a,n}^{(t)}$, which is the access traffic demand on UAV-BS n (see (1)), is given by:

$$b_{a,n}^{(t)} = \sum_{u \in \mathcal{U}_n^{(t)}} l_u^{(t)} \qquad l_u^{(t)} \geq 0, \forall n \in [1, N] \tag{5}$$

Traditionally, when the MEC technology is not employed, $b_{a,n}^{(t)} = b_{BH,n}^{(t)}$, since the traffic demand of each user is transmitted in the access, as well as in the BH networks. Nevertheless, when MEC is used, i.e., a caching server is installed on each UAV-BS n, the situation is different. In case a user u is associated to an UAV-BS n and he/she requires a content which is stored on that UAV-BS, that content is not transmitted in the BH network, but is directly sent to the user. As a result, the traffic demand in the BH network is:

$$b_{BH,n}^{(t)} = p_{miss} \sum_{u \in \mathcal{U}_n^{(t)}} (\lfloor \frac{l_u^{(t)}}{S} \rfloor \cdot S) + \sum_{u \in \mathcal{U}_n^{(t)}} (l_u^{(t)} \mod S) \tag{6}$$

As derived from (4), the miss probability p_{miss} is 1 if the MEC technology is not employed and it decreases with the growth of the server capacity. Knowing this, (6) shows that the MEC technology and the rise of its size prevent the BH network from congestion, since $b_{BH,n}^{(t)}$ linearly drops with p_{miss}.

3.3. Power Consumption Modelling

The network power consumption at time t is the total power consumption of the wireless network, considering the power

needed to provide the access, BH and caching features in the network, at time t:

$$P^{(t)} = \sum_{n=1}^{N} \left(P_{a,n}^{(t)} + P_{BH,n}^{(t)} + P_{c,n}^{(t)} \right) \quad (7)$$

where $P_{a,n}^{(t)}$, $P_{BH,n}^{(t)}$ and $P_{c,n}^{(t)}$ are the access, BH and caching power consumption of each UAV-BS n during time slot t. If UAV-BS n is not active, $P_{a,n}^{(t)}$, $P_{BH,n}^{(t)}$ and $P_{c,n}^{(t)}$ are considered zero. The LTE power consumption models, in watt, for the access and BH networks, for each UAV-BS n are based on [5] and [62]:

$$P_{a,n} = n_{sec} \cdot \left[P_{DSP} + MIMO_{Gain} \cdot \left(P_{trans} + \frac{P_T}{\eta} \right) \right] \quad (8)$$

$$P_{BH,n} = P_{DSP} + MIMO_{Gain} \cdot \left(P_{trans} + \frac{P_T}{\eta} \right) \quad (9)$$

where n_{sec} is the number of sectors of the access network, P_{DSP} is the Digital Signal Processor (DPS) power consumption in watts, the $MIMO_{Gain}$ is the MIMO gain of the transmitter, the P_{trans} is the power used by the transceiver, the P_T is the actual radiated power by the antenna and η is the power amplifier efficiency. The power consumption needed for the cache server supply $P_{c,n}^{(t)}$ of each UAV-BS n, in watt, is modelled as in [41] and [61]:

$$P_{c,n}^{(t)} = \omega_{MEC} \cdot C \cdot S \quad (10)$$

where ω_{MEC} is expressed in W/bit, C is the capacity of the server, expressed in maximum number of files, which can be stored and S is the size of each file, in bits. In the computation, the power needed by an UAV-BS for flying is not considered.

3.4. Time Delay modelling

We model the transmission time as the delay cost. As previously mentioned, in case a user u needs a content which is stored locally on the UAV-BS n with which he/she is associated, that content is directly sent to him/her. If this is not the case, the content is retrieved in the cloud, reached through the BH network. The average transmission delay is:

$$D = p_{hit} \cdot D_{hit} + (1 - p_{hit}) \cdot D_{miss} \quad (11)$$

where for p_{hit} is given by (4). D_{hit} is the time needed to send a content from an UAV-BS to a user and D_{miss} is the time needed to bring a content from the cloud to a user. This results in $D_{hit} < D_{miss}$ and, hence, from (11), the growth of p_{hit} makes D drop. As already mentioned and highlighted in (4), p_{hit} grows with the growth of the number of stored contents C, i.e. the cache capacity.

3.5. Traffic Demand Modelling

We first analyse and model the traffic demand during public events, as football matches, concerts, and so on. To do this, we use data provided by a large Italian mobile network operator. These data report the traffic demand volume, in bits, of 1420 BSs located in the city of Milan (Italy) and in a wide area around it, for two months in 2015, with granularity of 15 minutes. First, we update the value of the traffic based on the average increment, equal to 7.5 times, of the mobile market in Italy from 2015 to nowadays, as reported in [63]. Then, we transform the traffic volume in bit rate, normalising the values by the granularity of samples, i.e., 15 minutes. Then, we select the trace corresponding to BS close to the soccer stadium of San Siro, which often hosts public events, and we investigate its traffic profile. Each coloured curve in Fig.2a shows the bit rate, in Mbps, of each match, that took place there during the Spring of 2015. The black circle marked line is the mean bit rate in each 15-minutes long time interval, computed using the whole traffic trace. These matches started at 8.45 p.m., marked by the dashed black line on the left and their intermission began at 9.30 p.m., indicated by the other black dashed line. From the figure, it is visible that the traffic demand significantly increases during matches with respect to the average traffic demand (black line in Fig.2a). Then, we also notice that, the bit rate during each event typically starts growing prior to the beginning of a match. Shortly before the kickoff, it slightly decreases and when the intermission starts, the traffic demand always presents the peak, decreasing again as soon as the match resumes.

Table 2
Summary of the traffic model notation.

Notation	Definition
$\beta^{(t)}$	Bit rate at time t
$\beta_{Avg}^{(t)}$	Average bit rate at time t
β_{Peak}	Bit rate at the peak
$U^{(t)}$	Shape function,
$K^{(t)}$	Scalar to scale the average traffic demand
λ	Parameter of the exponential distribution
$\lambda_u^{(t)}$	Bit rate of user u at time t
Λ_{Avg}	Average traffic volume of a user at the peak
U	Number of users

To shape this behaviour, we assume that the bit rate $\beta^{(t)}$, at time t, is given by:

$$\beta^{(t)} = \beta_{Avg}^{(t)} \cdot U^{(t)} \cdot K^{(t)} \quad (12)$$

where $\beta_{Avg}^{(t)}$ is the average bit rate, in Mbps, see black circle marked line in Fig.2a; $U^{(t)}$ is a shape function, used to model the trend of the bit rate during each event and $K^{(t)}$ is a scalar, which scales the average traffic demand. In order to build the $U^{(t)}$ function, we normalise the piece of each bit rate trace corresponding to each match, reported in Fig.2a, by its peak. Then, we average these normalised bit rates, time interval by time interval, to obtain its average shape during a public

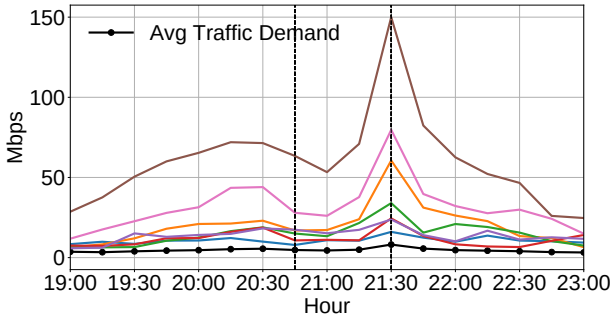

(a)

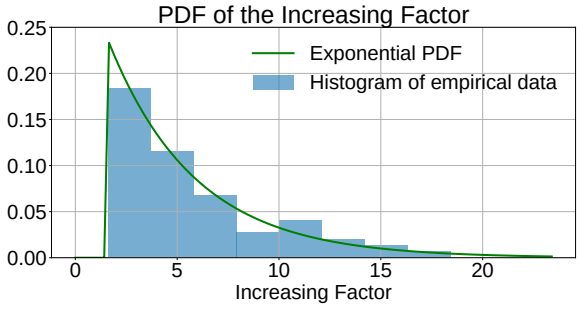

(b)

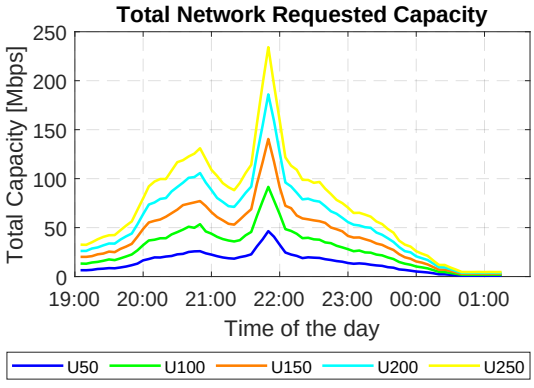

(c)

Figure 2: Traffic Analysis, Modelling and Generation: (a) Traffic demand, in bits, during public events at the San Siro soccer stadium, (b) PDF of the Increasing Factor, (c) Requested capacity for an average value of 0.24 for different users scenarios. U:Users

event. In the end, in order to determine the value of $K^{(t)}$, we collect the increasing factors for each bit rate sample, with respect to the average. This means that each $K^{(t)}$ is computed as $\frac{\beta^{(t)}}{\beta^{(t)}_{Avg}}$, where $\beta^{(t)}_{Avg}$ is as previously discussed. The Probability Density Function (PDF) of these $K^{(t)}$ is reported in Fig.2b, where in blue there is the histogram plot of these data, while the green line is the PDF of an exponential distribution that best fits it, whose parameter is λ=0.24. As a result, assuming that the number of users remains constant during the event, the bit rate of each user u, $\lambda^{(t)}_u$, from which it is possible to derive the traffic demand volume $l^{(t)}_u$ discussed

Table 3
Summary of the channel model notation.

Notation	Definition
$\mathcal{N}$	Normal Distribution for the excess path loss for the access network
μ	Mean of $\mathcal{N}$
σ	Standard Deviation of $\mathcal{N}$
θ	Elevation angle between users and UAV-BS
a	Frequency parameter for access PL model
b	Environmental parameter for access PL model
d_{3D}	3D distance between TBS and UAV-BS
f_c	Central frequency of the BH PL model
h_{TBS}	Height of the Terrestrial BS

in section 3, is as follows:

$$\lambda^{(t)}_u = \Lambda_{Avg} \cdot U^{(t)} \cdot K^{(t)} \tag{13}$$

where $U^{(t)}$ is computed as described above and $K^{(t)}$ is a sample extracted from an exponential distribution, with parameter λ equal to 0.24. Λ_{Avg} is the average traffic volume of a user at the peak and it is computed as $\frac{\beta_{peak}}{U}$, where β_{peak} is taken from data and it is 79.03 Mbps and U is 360. As a result, the total required bit rate is shown in Fig.2c, where each curve corresponds to a different number of users U. Observe that the shape of each curve well fits the typical behaviour which characterises the public events (see Fig.2a). The requested traffic presents a peak of 235 Mbps, in the scenario where there are 250 users, as can be noticed in Fig.2c.

3.6. Path Loss and Channel Modelling

Several path loss models are used to evaluate the aerial to ground communications as described in [64]. For the access network link, we consider the aerial to ground model from Al-Hourani et al. [65], which offers a statistical path loss model for sub-6GHz bands. It is based on the Free Space Path Loss (FSPL) model using ray tracing for urban and suburban environments accounting for the effects of buildings into the model. The Al-Hourani path loss model is described in (14), where FSPL is the free space path loss model from the Friss equation. $\mathcal{N}$ is the normal distribution for the excess path loss with a mean of μ, and standard deviation σ as expressed in (15), where a and b are frequency and environment-dependent variables and θ is the elevation angle between the ground and the aerial nodes. This model is suitable for urban environments with building representation. To account for that, we use the model in the 2.6 GHz band setting the μ, a and b values to 1.67, 8.59 and 0.04 for the Line-of-Sigh (LoS) model, while the values for the Non-Line-of-Sigh (NLoS) are 18, 26.53 and 0.003 respectively.

$$PL_{Access} = FSPL + \mathcal{N}(\mu, \sigma^2) \tag{14}$$

$$\sigma = a \cdot e^{(-b \cdot \theta)} \tag{15}$$

For the BH network we consider the TR 36.777 path loss model since is more suitable for the communication between terrestrial base station (TBS) and aerial nodes in the 3.5GHz band [66]. This model is suitable for antennas higher that 22 m and distances up to 4km. In (16) we described the LoS path loss model where d_{3D} is the three-dimensional distance between the TBS and the UABS and f_c is the central transmission frequency. The NLoS path loss model is described in (17) where h_{TBS} is the height of the TBS. Detailed parameters of the link budget that influence the channel model are described in Table 4 of Section 4.2.

$$PL_{BH_{LoS}} = 28 + 22log_{10}(d_{3D}) + 20log_{10}(f_c) \tag{16}$$

$$PL_{BH_{LoS}} = (46 - 7log_{10}(h_{TBS}))log_{10}(d_{3D}) + 20log_{10}\left(\frac{40\pi f_c}{3}\right) - 17.5 \tag{17}$$

4. Methodology

4.1. Scenario Definition

In previous sections of this work, we consider a crowded environment, located in an area of 1 km^2, delimited in orange in Fig.3, situated in the city centre of Ghent, in Belgium, and we assume that the typical yearly festival is taking place. The total event duration is 6 hours, from 7 p.m. to 1 a.m., where users are arriving progressively at the main events at 9 p.m. and 10 p.m. In order to evaluate the density of users rather than the actual size of the city, we evaluate the network in an area of 1 km^2, where the number of users will determine the density of users per km^2. The figure shows the city centre with 250 uniformly distributed users accessing the aerial network at the event time. Red crosses depict the unconnected users while green stars the connected ones. The drone icon defines the location of the serving UAV-BSs that fly at an elevation of 80 m [17] and the orange triangle presents the deployed facility, that could be a crane with a 60 m antenna or a traditional terrestrial BS, that is used by each drone to reach the BH network.

4.2. Network Architecture

We contemplate an UAV-BS aided network to support a crowded scenario, like a soccer match or a festival with realistic data requirements from ground users. Similarly to [5, 13, 17], the structure of the network is the one shown in Fig.1. The ground users access the communication service through the access network (orange links in Fig.1), provided by UAV-BSs, acting as traditional BSs. These UAV-BSs reach the CN, by BH links (blue links in Fig.1). Each BS equipment is mounted on a quadcopter MD4-1000, which can carry wireless communication equipment for more than one hour of flight time. These drones have a maximum speed of 45 km/h powered by a 22.2 V battery with a capacity of 17.33 Ah [67]. As described in [17] and [68], the connection between the UAV-BSs and the CN for a fast deployable network is given by an antenna on a truck or on a crane to increase its height, as shown in Fig.1. This facility can provide up to 25 simultaneous drones, and up to 500 battery packages to rapidly replace drones that are running out of energy, allowing the system to maintain up to 25 simultaneous UAV-BSs with nearly 20 takeovers per drone.

Figure 3: Scenario for the city centre of Ghent with 250 users

In the considered network, the height of this antenna is 60 m to avoid the majority of the building heights in the centre of Ghent [17]. LTE release 14 working on the 3.5 GHz band is used for the BH links with a bandwidth of 20 MHz consisting of 100 RB [69, 70, 71]. The access network uses a 2.6 GHz LTE femtocell based technology. Because of the static behaviour of the ground users, which is described in the following section, handovers and frequency allocation analysis are not considered in this architecture. Details of the access architecture can be found in [5] and the network simulation parameters are summarised in Table 4.

We assume that each UAV-BS is equipped with a MEC server, that provides the caching capability. Similarly to [61], the hardware technology of each cache is DRAM (Dynamic Random Access Memory). These servers update their contents according to the Least Frequently Used (LFU) cache algorithm, to store the most popular contents of the file library composed of 1000 files, as in [8, 10, 12, 38, 72, 73], of 50 Mbit size each [41, 42]. When a user requires a content, that is cached on his/her UAV-BS, the content is directly sent to that user, without retrieving it from the content provider nor accessing the BH network. Each of the UAV-BS locations is characterised by a specific order of popularity of contents. As in our model, the popularity is described by a Zipf's distribution [40, 9, 41, 61, 42]. The level of popularity of each content on each UAV-BS is determined from a reference popularity and, in order to introduce some slight differences among the file's popularity at different locations, i.e., at different UAV-BSs, random shuffles are performed at

Table 4
Link budget parameters for simulation [5, 17]

Parameters	Unit	Access	BH
Frequency	GHz	2.6	3.5
Bandwidth	MHz	5	20
Max Tx Power	dBm	33	43
Antenna Gain	dBi	4	5
Antenna Height	m	1.5	60
Noise Figure	dB	8	5
Fade Margin	dB	10	10
Shadowing Margin	dB	8.2	8.2
Interference Margin	dB	2	0
MCS and SNR	dB	1/3 QPSK = -1.5 1/2 QPSK = 3 2/3 QPSK = 10.5 1/2 16-QAM = 14 2/3 16-QAM = 19 1/2 64-QAM = 23 2/3 64-QAM = 29.4	

each server [8]. In particular, sorting the files of the library from the most popular to the least popular, according to this reference popularity, the popularity of 30% of the content is randomly swapped to generate the popularity on each UAV-BS.

4.3. Deployment Tool

In this paper, we conceive a java-based simulator based on [5, 17] for dynamic traffic scenarios. This tool accounts for the 3D city environment, users locations, traffic profile and network parameters to allocate users to specific UAV-BS. Each simulation covers an operating time of 6 hours, from 7:00 p.m. to 01:00 a.m.. Time uses 5 minutes long time slots.

In Fig.4 the full network allocation algorithm used in the simulation tool is depicted. First, the real 3D shape of the buildings located in the city centre of Ghent is read from a shape file, which describes that area (Box 1 in the figure). In this stage, the position of each user u is determined: his/her 3D coordinates (x_u, y_u, z_u), located inside the yellow area depicted in Fig.3, are determined. The position of each user is assumed static, meaning that it remains the same for the whole simulation, i.e. for the whole duration of the public event. This is a realistic assumption for the overcrowded scenario which we are considering, such as festivals and sport events, where users either maintain their position or move at a very slow pace. As in [74], these coordinates are assumed to be uniformly distributed over the considered area, since in this scenario, attractions are uniformly distributed in the considered area, resulting in an uniform distribution of users, meaning that each location has the same chance to be chosen as a possible location for the user. Once the position of each user has been generated, a set of possible location for the N UAV-BSs is created. This is done, by creating an aerial 3D-Grid where UAV-BS could hover. There are as many grid points as ground users. Each grid point uses the same (x_u, y_u) coordinates and (z_b) is set to 80 m or above if a building is present.

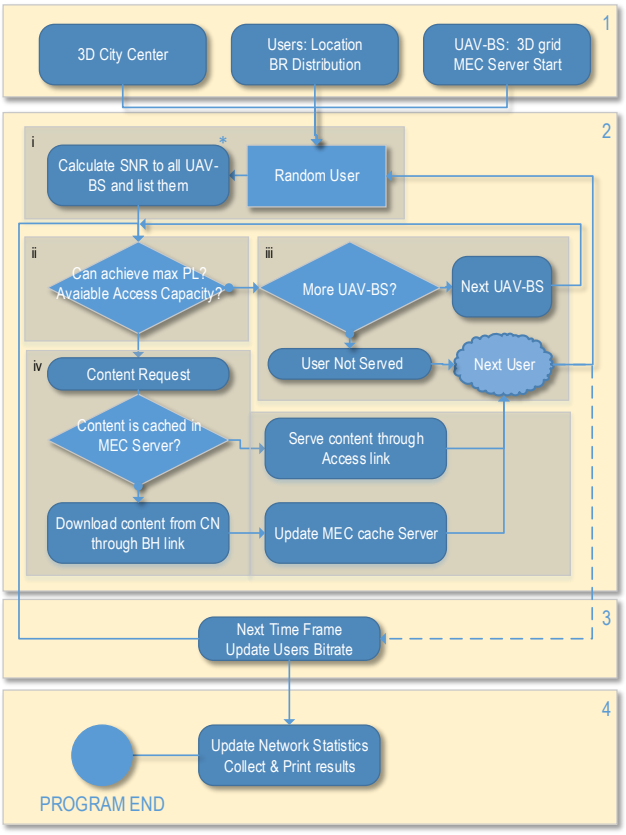

Figure 4: Network allocation algorithm of the tool

Now the actual simulation can start. For each time slot t, the bit rate experienced by each user is determined, using the model described in section 3.5. Then, each user is associated to an UAV-BS, if possible, and if this the case the required contents are delivered. Once each user is located and his/her traffic is determined, the procedure to associate, if possible, each user to an UAV-BS starts (Box 2 in Fig.4). For each user, the SNR to all the possible UAV-BS in the aerial network is calculated and organised. This step (i) is only done in the first time frame since all the users' and drone's locations are fixed. In the next step (ii), the algorithm calculates if the SNR is sufficient to connect the user to the selected UAV-BS adjusting the transmitting power. Then it calculates if the UAV-BS has available access capacity for the requested bit rate. If one of these parameters is not achieved (step iii), the algorithm selects the next UAV-BS in the list to repeat step ii or proceed to the next user if the actual is unable to be served. Further, if the bit rate can be served (step iv), the content manager evaluates if the content is cached in the MEC server of the UAV-BS. If it is cached, it is delivered to the user through the access link. If not, it is downloaded from the cloud through the BH link and then saved in the MEC cache server. Once all the users are evaluated, the algorithm proceed to the next time frame, updating the bit rate of all the users (Box 3). All the steps from stage 2 are repeated except from step i, since all the locations are static.

Details of the network generation and content delivery are described in sections 4.3.2 and 4.3.3 respectively. Finally, all the statistics are calculated and collected for presenting the results in spreadsheet files for further analysis (Box 4). Details of each step are given in the following subsections.

4.3.1. Dynamic traffic generation

At the beginning of each time slot t, $\lambda_u^{(t)}$, the bit rate of each user u, is determined. To do this, we use the model discussed in section 3 and in (13). From the bit rate $\lambda_u^{(t)}$, the traffic demand volume $l_u^{(t)}$ is derived and the number of content requests is computed as $\lfloor \frac{l_u^{(t)}}{S} \rfloor$, where S is the size of each content, which is 50 Mbit, as in [41].

4.3.2. Network Generation

In this step of the simulation, each user is associated to an UAV-BS, if possible. Before starting this procedure, for each user, which contents are requested is determined. To do this, for each user, the path loss experienced from each UAV-BS is computed as in [17], taking into account the presence of the real buildings in the area, whose shape is provided to the simulator, as mentioned above. Then, the content popularity of the UAV-BS, which provides the lowest path loss, is picked and used to determined which contents that user requires.

At this point, the association procedure begins. The list of active UAV-BS is generated, to which the user u can be connected. A BS is inserted in the list, if the experienced path loss is lower than an allowable maximum and it can provide the requested traffic demand in the access and BH network. The path loss has to be lower than the maximum allowable, in order to guarantee to the user to receive the signal with a sufficient quality. If the experienced path loss is greater than the allowable maximum, the input power of the UAV-BS is increased until it becomes acceptable. In case the input power reaches the maximum allowable input power, but the path loss is still larger than the maximum, that UAV-BS is not inserted in the list. The user traffic demand in the access network is $l_u^{(t)}$, or $\lambda_u^{(t)}$ if expressed in bit rate. This means that an UAV-BS n is able to provide the required traffic demand in the access network, if the following condition is verified:

$$l_u^{(t)} + \sum_{v \in \mathcal{U}_n^{(t)}} l_v^{(t)} \leq B_a \tag{18}$$

where $\mathcal{U}_n^{(t)}$ is the set of user already associated with UAV-BS n, $l_v^{(t)}$ is their traffic demand and B_a is the maximum access traffic volume, which is, assuming that its maximum bit rate is 16.9 Mbps, $5.07 \cdot 10^3$ Mb, since each time slot lasts 5 minutes. The traffic demand in the BH network depends on the contents, which are requested by the user and which are stored on the considered UAV-BS n. Indeed if a requested content is stored on that UAV-BS n, in case that user is associated with n, that content is directly sent to the user and the BH network is not used for its delivery. As a result, in order to verify if an UAV-BS n is able to carry the needed traffic demand at time t in the BH network, the following condition is verified:

$$(l_u^{(t)} - Hit_u \cdot S) + \sum_{v=1}^{N} b_{BH,v}^{(t)} \leq B_{BH} \tag{19}$$

where Hit_u is the number of contents which are requested by user u and stored in the UAV-BS n, S is the size, in bits, of each content, assumed 50 Mbit, N is the number of UAV-BSs, B_{BH} is the maximum BH traffic volume in a time slot 5 minutes long, set equal to $21.6 \cdot 10^3$ Mb, assuming that its maximum bit rate is 72 Mbps. Notice that in order to compute Hit_u, we are optimistically assuming to perfectly know which contents are requested by user u. To overcome this assumption, the prediction of the content requests is needed, which typically uses Machine Learning-based approaches or Lagrange interpolation, as in [75, 76]. Nevertheless, without loss of generality, this is out of the scope of this work, and we leave it as future work. Then, $b_{BH,v}^{(t)}$ is the sum of the traffic demand of the set of users $\mathcal{U}_v^{(t)}$ associated with UAV-BS v during the time slot t:

$$b_{BH,v}^{(t)} = \sum_{v \in \mathcal{U}_v^{(t)}} (l_v^{(t)} - Hit_v \cdot S) \tag{20}$$

where $l_v^{(t)}$ is the traffic demand at time t of each user v, as above, Hit_v is the number of contents which are requested by user u and stored in the UAV-BS v and S is 50 Mbit.
Summarising, if an UAV-BS transmits and the user receives the signal with acceptable quality, i.e. with acceptable path loss, and UAV-BS satisfies (18) and (19), that UAV-BS is inserted in the list. The user is associated to the UAV-BS from which he/she experiences the lowest path loss among the UAV-BSs in the list. In case the list results empty, the same procedure is performed using only the inactive UAV-BSs. In case also this provides an empty list, the user remains uncovered.

4.3.3. Content Delivery

In each time slot t, once each user has been associated with an UAV-BS n, if possible, the requested contents are delivered. As already mentioned, if a content f, requested by the user u, is cached in the serving UAV-BS n, a hit occurs: the content is directly transmitted to the user. In case of miss, i.e. the required content is not cached at the UAV-BS n, the content is retrieved from the content provider, reached by the CN, accessed through the BH network. We assume that each requested content is transmitted at the minimum bit rate which allows to receive it within a time slot, i.e. 0.17 Mbps, independently on the required bit rate $\lambda_u^{(t)}$. As a result, the transmission time in case of hit, similar to [41], is:

$$D_{Hit} = \frac{S}{\lambda_S} \tag{21}$$

where S is 50 Mbit and λ_S is 0.17 Mbps. In case of miss, the transmission time is the transmission time in the access network, in the BH network and in the CN:

$$D_{Miss} = D_a + D_{BH} + D_{CN} \tag{22}$$

where D_a is, as in (21), is the time needed to transmit the content from the UAV-BS to the user; D_{BH} is the transmission time in the BH network. We assume that the bit rate for the download in the BH network is λ_S equal to 0.17 Mbps, but this is increased when the allocated bit rate in the BH network, for the UAV-BS n, given by the bit rate in each allocated RB, is larger than the needed:

$$D_{BH} = \frac{S}{(\lambda_S + \frac{1}{miss_n^{(t)}}(RB_n^{(t)} \cdot \beta_{RB} - b_B^{(t)} H, n)} \quad (23)$$

where S is 50 Mbit, $miss_n^{(t)}$ is the number of miss at time t, on UAV-BS n, i.e. the number of requests which need the BH network to retrieve the content, λ_S equal to 0.17 Mbps, β_{RB} is the bit rate per RB, equal to 0.72 Mbps, $RB_n^{(t)}$ is the number of RB which are used by UAV-BS n at time t. D_{CN} is the time needed in the CN and, as in [9, 18], is 50 ms. Once each requested content is delivered, each cache is updated, according to the Least Frequently Used (LFU) cache algorithm, so as to always cache the most popular contents.

5. Key Performance Indicators

The performances of the proposed methodologies are evaluated using the KPIs described below.

Capacity

The capacity of the network is defined as follows:

- Access Capacity: This is the total used access capacity of the network in a time slot, measured in Mbps.
- BH Capacity: This provides the total used BH capacity during a time slot, in the network, in Mbps.
- Number of Used Resource Blocks: This is the total number of used RBs in the network.

If we want to measure the capacity globally, we measure the access and the BH capacity which is used during the whole duration of the event in each simulation. In order to distinguish from the previous KPIs, we name them *total Access Capacity* or *total BH Capacity*, respectively.

Provisioned Users

The percentage of Provisioned Users corresponds to the percentage of served users, during each time slot of each simulation. A user is considered provisioned if he/she can be associated with an UAV-BS, i.e. if there is at least an UAV-BS, from which the experienced path loss is lower than the maximum allowable path loss and has enough available access and BH capacity to provide the required bit rate.

Average Power Consumption

The average Power Consumption is the power consumption of the wireless network, averaged over the time, considering the power needed in order to provide the Access, BH and caching features in the network:

$$P = \frac{1}{T} \sum_{t=1}^{T} P_t \quad (24)$$

where P_t is the power consumption in time slot t, computed as in (7), which sums the power needed by each UAV-BS to provide the access and BH networks, as well as the caching feature.

UAV-BS

The UAV-BS provides the number of UAV-BS locations needed during each simulation.

Average Transmission Time

As in [51], we use the average transmission time, defined as the time needed to retrieve each requested content, given by:

$$D = \frac{1}{\sum_{t=1}^{T} U^{(t)} \sum_{u=1}^{U^{(t)}} R_u} \sum_{t=1}^{T} \sum_{u=1}^{U^{(t)}} \sum_{r=1}^{R_u} d_{u,r} \quad (25)$$

where $d_{u,r}$ is the transmission time for the content request r, requested by the user u and is computed as in (21) and (22). R_u, $U^{(t)}$ and T correspond to the number of requests required by the user u, the number of served users at time t and the duration of the simulation, respectively.

6. Results

The results are evaluated varying the capacity of each MEC server and for different values of the parameter α, characterising the contents' popularity distribution. The effects of the growth of the user density, from 50 to 250 $users/km^2$ are also investigated. First, we analyse the capacity of the access and BH network following by the covered users. Next, the delay performance of the cache system is described after presenting the evaluation of the network power consumption. Finally, we discuss the impact of the user density on our system proposal.

6.1. Access and BH Capacity

Figs. 5a, 5b and 5c show the behaviour of the used access, BH capacity, and the number of BH RBs, respectively, with 250 $users/km^2$, considering the α parameter to describe the popularity of contents. In these figures, α equal to 1.06, an average value for the Zipfs's distribution. The dashed line is the total required bitrate and each of the other curves corresponds to the used access and BH capacity, with a different capacity of each MEC server, measured in percentage of the library that the server can store. If it is equal to 0%, we are considering the scenario that does not use the MEC technology. In this case, each content requested needs to access the CN, through the BH link in order to retrieve the file. This means that the BH bitrate needed by each user corresponds to the total bitrate required by that user.

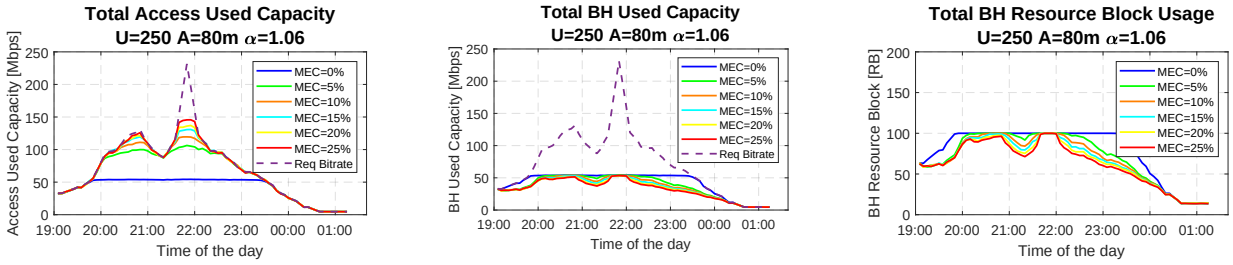

(a) (b) (c)

Figure 5: Used capacity with α equal to 1.06: (a) Used Access Capacity (Mbps), (b) Used BH Capacity (Mbps), (c) Used BH RBs. MEC=XX%: MEC Server cache size (%). U:Users. A:Altitude

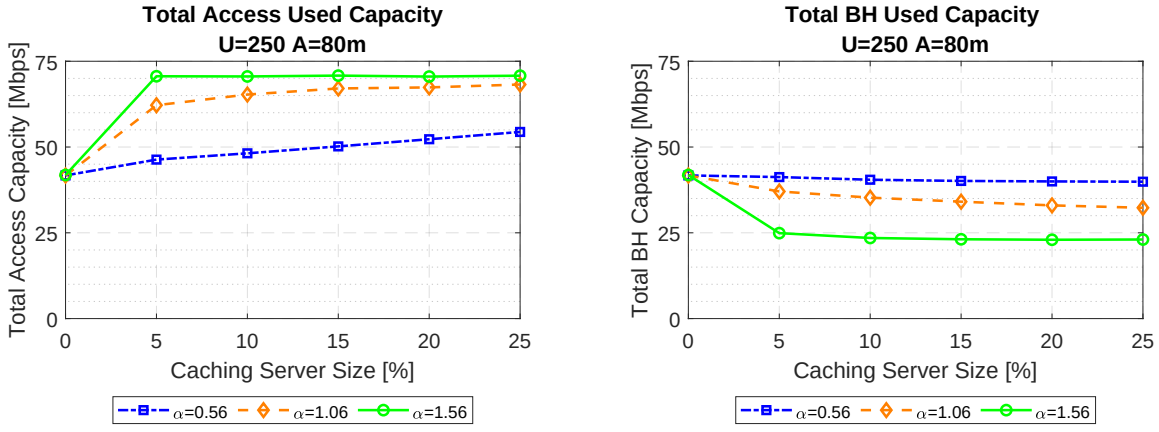

(a) (b)

Figure 6: Used capacity varying the Size of MEC Server (a) Access Link (Mbps), (b) BH Link (Mbps). U:Users. A:Altitude

From Fig.5a, it is possible to notice that, until 19:50, the used access and BH capacity, given by the blue curve, respond instantaneously to the required bitrate. Then, at 19:50, the used access and BH capacity, become flat and are unable to provide the required bitrate (dashed curve in Fig.5b). This is because the available RBs are totally used (Fig.5c), which means that the BH network is saturated. After the peak, the traffic demand decreases. After 23:10, traffic demand is so low that not all the BH RBs' are needed. This means that the network is not saturated anymore and can provide the required bitrate.

When the MEC technology is used, i.e. the capacity of each server is larger than 0%, the used BH capacity, as well as the number of used RBs, is lower than the case without the MEC technology. This is because, part of the contents that are requested by the users are stored locally, in the MEC server. Thus, in case of a hit, retrieving the content at the content provider, reachable through the BH network, is not needed. This occurs more often with larger cache size, since finding the requested content locally stored is more likely. For this reason, the BH used capacity, as well as the number of used BH RBs, is lower if larger caches are considered. The used access capacity is larger, since the BH network is prevented from saturation: when the required bitrate becomes significantly large, from 19:50 on, not all the RBs are used. Nevertheless, when the required bitrate reaches the peak, at 21:45, the BH network saturates, i.e., the needed RBs are larger than the available ones, and for this reason the used access capacity is between 50% and 80% of the required bit rate, depending on the size of the MEC server installed on each UAV-BS.

In Figs. 6a and 6b, the averaged used access and the BH capacity during the whole intervention are shown varying the capacity of each MEC server, respectively. The blue, orange and green curves provide the used access and the BH capacity, with α equal to 0.56, 1.06 and 1.56, respectively. From the figure it is clear that, as already seen in Fig.5, increasing the size the MEC server installed on each UAV-BS determines the growth of the used access capacity and the drop of the used BH capacity. This is because if more contents are locally stored, the need to retrieve the content in the cloud is less likely, and, as consequence, less capacity is needed in the BH network, avoiding its saturation and permitting to use more capacity in the access one. Nevertheless, as can be observed in Fig.6, the trend of the capacities strictly depends on the parameter α, characterised by the Zipf's distribution, used to describe the popularity of files. Large values of α means that there is a small part of the library which

is very popular. If this is the case, even a small cache significantly increases the used access capacity, while decreasing the needed BH capacity. This occurs when α is larger than 1: the used access capacity is larger than 60 Mbps and the BH capacity is not larger than 24 Mbps if only 5% of the library is locally stored. In case of a small value of α indicates that the files have similar popularity. In this case, larger caches are needed to significantly increase the used access capacity and decrease the used BH one: if the popularity distribution parameter α is equal to 0.56, 15% of the library should be stored to use 50 Mbps as the capacity of the access network. With respect to the BH network capacity, it is not significantly reduced, even if 25% of the library is locally stored, i.e. from 41 Mbps, when the MEC technology is not used, to 40 Mbps. when the cache capacity is 25% of the library. As an example, when the caching server is deactivated, the access and BH capacity are the same (41.8 MBps), but will represent 58% of the BH and only an average of 25% of the access network, and will vary depending on the number of active UAV-BS used.

6.2. Provisioned Users

In this subsection, we discuss the effects of the MEC technology on the user coverage. Fig.7a shows the percentage of provisioned users versus the capacity of each MEC server, for three different values of α in the scenario with 250 users/km^2. From the figure, it is visible that the growth of the cache capacity installed on each UAV-BS determines the improvement of the number of provisioned users. If larger caches are used, storing locally a requested content is more likely. This means that, more likely, the access to the cloud to retrieve that content is unneeded and less BH capacity is employed. As a consequence, the whole network does not saturate and more users can be served. When the MEC technology is not employed, i.e. each MEC server stores 0% of the file library, all the bitrate required by each user has to be provided in both access and BH network. This makes the BH network more exposed to saturation, resulting in less than 75% of provisioned users. In this case, the BH network saturates as soon as the traffic demand reaches nearly 54 Mbps (see Fig.5a). The MEC technology prevents the BH network from this, making the user coverage improved. This improvement highly depends on the distribution of contents popularity. When there is a small group of very popular contents, ($\alpha > 1$) between 93% and 99% of the users is covered, when only 5% of the library is locally stored, since it is more likely that the required contents are cached. In case all contents have similar popularity, since requesting for a cached content is less frequent, larger capacity of the MEC servers is needed in order to significantly improve the provisioned users: when 10% of the library is locally stored, 80% of the users is provisioned.

A more detailed analysis of the peak hour and the provided users is found in Fig.7b, where the percentage of served users versus time is shown for different values of the MEC servers' capacity. Typically, at the beginning of each simulation 100% of users are provisioned, but as soon as the

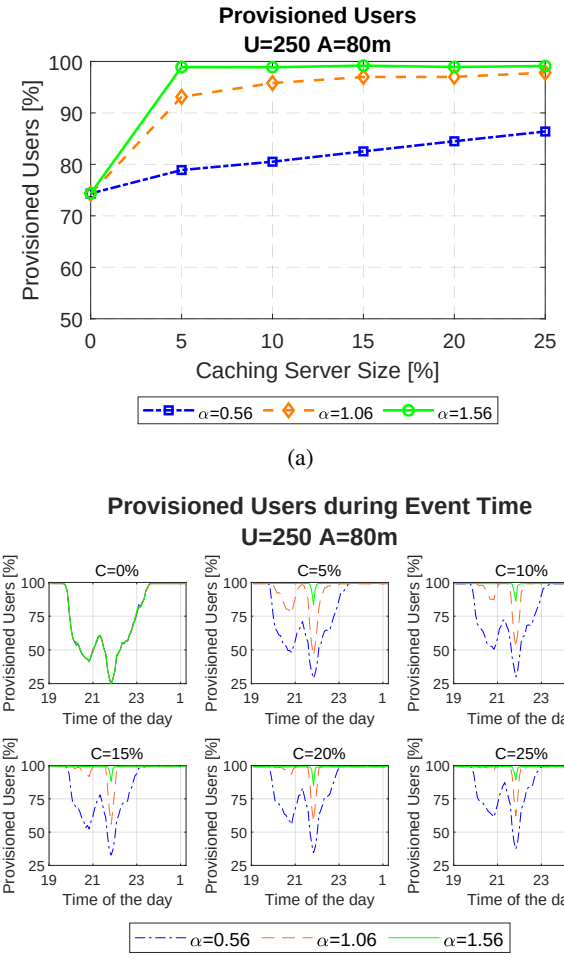

Figure 7: Percentage of Provisioned Users (%) compared with α and MEC server size (a) Averaged for whole event, (b) Plot in time. C=XX%:MEC Server size (%). U:Users. A:Altitude.

required bitrate increases, the benefits provided by the employment of the MEC technology are more evident. When MEC is not used (MEC server capacity = 0%), the provisioned users are significantly reduced. When the traffic demand reaches its peak, at 21:45, without MEC technology, only 23.5% of users are provisioned. These are between 28.8% and 37.3%, if MEC server are installed on each UAV-BS and contents have similar popularity, i.e. if α is 0.56. Up to 83.7% and 89.2% of users are served during the peak if α is larger than 1 for MEC capacities of 5% and 25%, respectively. However, for $\alpha = 0.56$ the enhancement was not so good; as shown by the blue lines in Fig.7b several users remain unconnected at the beginning of the match and in the half time break. At this peak periods, the served users ranges between 28.8% to 37.3% for the different sizes of the MEC server.

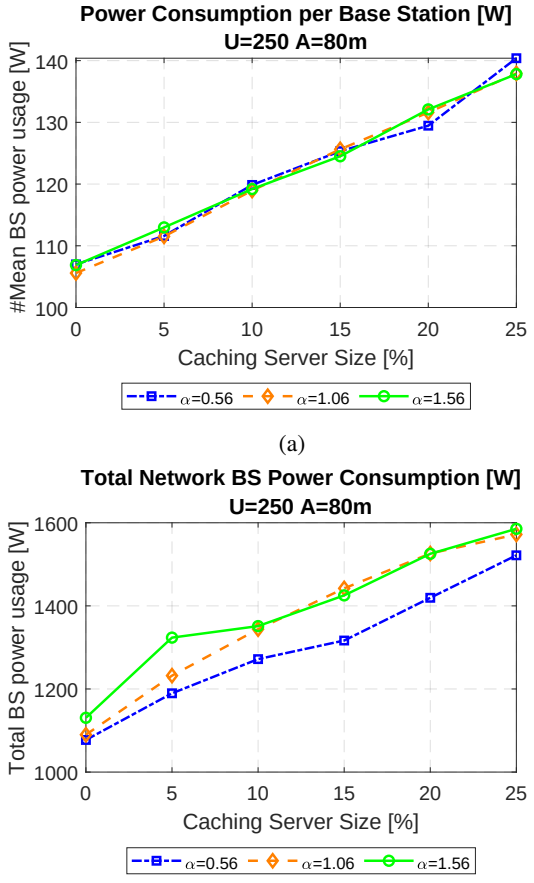

Figure 8: Power consumption analysis: (a) Total power consumption for the whole network, varying the capacity of each MEC server, (b) Averaged Power consumption per Base Station, U:Users. A:Altitude.

6.3. Power Consumption

From Fig.8a, the power consumption of each UAV-BS presents a simple linear behaviour only dependant on the size of the MEC server. It is given by the average power needed by each UAV-BS to provide the access and BH links, as well as the power required for the MEC server during each simulation. The results highlights that, as expected, the power consumption of each UAV-BS is not affected by the characteristics of the popularity of files distribution and it linearly increases with the MEC server capacity. This linear trend is due to the model of the MEC server power consumption which is used in our simulations, see (10). The power consumption increases by 12% if 10% of the library is locally stored and it grows up to 31% if each server stores 25% of the library, from 106 W when no caching is used, to 140 W.

Now, we investigate the impact of the usage of the MEC technology on the network power consumption, reported in Fig.8b, where each line is the average network power consumption for different values of the α parameter, varying the cache capacity of each MEC server. We notice that the network power consumption is slightly higher when the α parameter and/or the capacity of each cache server grows. Indeed, when each MEC server stored 5% of the library, it increases by 10%, 13% and 17%, when the α is 0.56, 1.06 and 1.56, respectively, with respect to the case with no MEC technology employment. This is because the number of UAV-BSs locations slightly increases with the cache capacity, as can be seen in Fig.9a, where the rise of the number of UAV-BS locations grows for larger values of the cache size and the α parameter. In particular, the average number of UAV-BSs locations increases from an average of 10.1 BSs for α and cache capacity equal to 0.56 and 0%, respectively to 11.4 BSs if they are 1.56 and 25%, respectively. By enlarging the cache size, a requested content is more likely to be already cached, so that less BH network capacity is needed, avoiding its saturation and permitting to use more access capacity. As soon as the access capacity of an UAV-BS is totally used, an unused UAV-BS can be activated, until the BH network saturates, generating a growth in the number of used UAV-BS locations, as well as of network power consumption. Despite that it seams that lower values of α consume less network power, the power efficiency of the network (*Eff*), defined as the averaged power of the network divided by the total number of served users, is higher for lower values of α, i.e. 18.5 $mW/user$, 17.1 $mW/user$ and 16.8$mW/user$ for α equals to 0.56, 1.06 and 1.56 respectively.

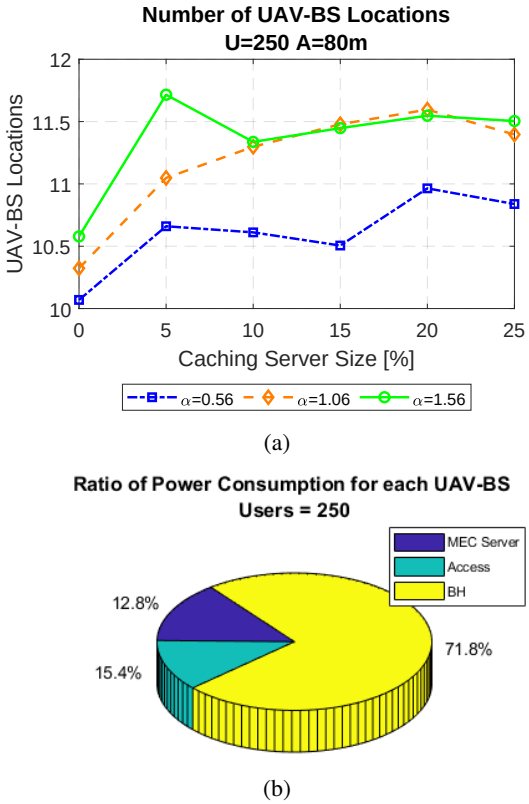

Figure 9: Power consumption analysis: (a) Number of employed UAV-BS locations, varying the capacity of each MEC server, (b) Power consumption ratio of different UAV-BS sections, U:Users. A:Altitude.

Fig.9b shows each power consumption contribution, distinguishing among the power needed to provide the communication (access and BH in green and yellow, respectively) and the caching, in blue, features. The total power consumption of an UAV-BS, 15.4% and 71.8% for the access and BH networks, respectively, while the latter for 12.8%. Even if the usage of the MEC technology impacts the power consumption of an UAV-BS, this does not determine a relevant UAV-BS flight duration reduction. It decreases by 10%: from 77 *min*, when no MEC servers are used, to 69 *min*, if the MEC server stores 25% of the library. Considering the duration of our event, which is 360 *min*, the drop of the flight duration of an UAV-BS determines the increase of the needed number of drones per location during the simulation from 5 to 6.

6.4. Average Transmission Time

Pushing caching resources closer to the users provides significant benefits in terms of reduction of the latency. Indeed, if a user requests a content which is locally stored, the BH and CN networks are not accessed and the transmission time is only the time needed to download the content from the UAV-BS. On the contrary, if that content is not locally cached, it is retrieved in the cloud. In this case, the content is downloaded from the cloud through the UAV-BS. The behaviour of the transmission time, while increasing the capacity of each caching server, installed on each UAV-BS is given in Fig.10, where each curve corresponds to a different value of α. The growth of the size of the cache generates reduction of the transmission time, from 500 s down to 458 s, 398 s and 329 s depending on the value of α in a 25% server size. Notice that, even if these values appear high, they are as expected, according to the computation of the experienced latency, see (21), (22). This reduction of the transmission time is because more contents can be stored locally and the access to the cloud is more likely unneeded reducing the transmission time to only the access network. Also in this case, this reduction strictly depends on the characteristics of the popularity, used to model the popularity of contents. For larger values α, even a small cache size drastically reduces the transmission time compared with the no MEC scenario. When α is 1.56, the transmission time is reduced by 25%, from 500 s to 375 s, with 5% of the library locally stored. A small value of α indicates that the files have similar popularity and the probability to take a content from the CN is higher. As a result, for α equal to 0.56, at least 20% of the library should be stored to reduce the experienced delay by 5% with respect to the no MEC technology usage.

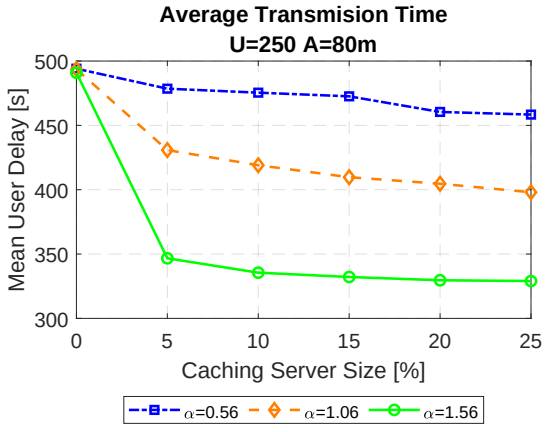

Figure 10: Average Transmission Time, varying the capacity of each MEC server. U:Users. A:Altitude.

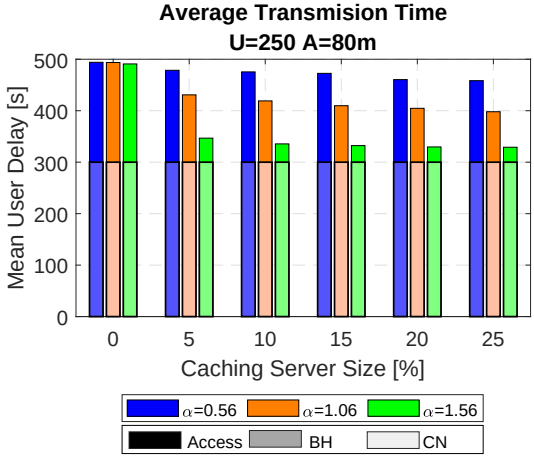

Figure 11: Average Transmission Time distinguishing between Access, BH and CN time, varying the capacity of each MEC server. U:Users. A:Altitude.

In Fig.11, the transmission time is reported, for different values of α, increasing the cache capacity. The average time needed in the access network is reported by the bars marked by dark colours, while the time needed in the BH network is indicated with the bars with light colours. Finally, the time needed in the CN is given by the bars with the clearest pattern. As in Fig.10, the average transmission delay drops if the cache capacity and/or the α parameter rises. Moreover, from Fig.11, we notice that the CN transmission time is negligible with respect to the access and BH network transmission delay. In addition, the access transmission delay remains constant, despite the growth of the cache capacity, as well as of the parameter α, which makes more likely the hit occurrences. Indeed, the drop of the average transmission delay is due to the drop in the average BH network transmission time. This is because, in case of a hit, which occurs more often with large cache capacity and α parameter, the resulting BH transmission delay is zero. This reveals that the MEC technology effectively reduces the transmission time through the reduction of the transmission time in the BH network, but the access transmission time bounds this reduction.

6.5. Variation of the number of users

In this part of the work, we provide an overview of the effectiveness of our methodology, varying the user density.

Each curve in Fig.12 corresponds to the percentage of provisioned users for different user density, from 50 to 250 $users/km^2$, increasing the capacity of each MEC server installed on each UAV-BS and using 1.06 as value of the

Table 5
Resume Results for Network Deployed With 250 Users

Indicator	Units	$\alpha = 0.56$			$\alpha = 1.06$			$\alpha = 1.56$		
Capacity of MEC	%	0	10	25	0	10	25	0	10	25
Coverage										
User Coverage	%	74.4	80.5	86.4	74.4	95.8	97.8	74.4	98.9	99.1
Total UAV-BS (Location)	-	10.1	10.6	10.8	10.3	11.3	11.4	10.6	11.4	11.5
Power Consumption										
Mean Power Consumption	W	11.2	23.7	42.4	11.2	23.7	42.4	11.2	23.7	42.4
Flight Time	min	76.9	73.8	69.6	76.9	73.8	69.6	76.9	73.8	69.6
Used Capacity										
Access Bitrate	Mbps	41.8	48.2	54.4	41.8	65.3	68.2	41.8	70.6	70.8
BH Bitrate	Mbps	41.8	40.5	39.9	41.8	35.2	32.3	41.8	23.5	23.1
Cache Bitrate	Mbps	0.0	7.7	14.5	0.0	30.1	35.9	0.0	47.1	47.7
MEC Usage										
Delay	s	497	475	458	494	419	398	490	335	329
Hit probability	-	0.00	0.30	0.42	0.00	0.63	0.71	0.00	0.87	0.88
Miss probability	-	1.00	0.70	0.58	1.00	0.37	0.29	1.00	0.13	0.12

α parameter. Fig.12 shows that, if no local caching is performed, (MEC server = 0%), the percentage of provisioned users, is dramatically affected by the network saturation as soon as the user density is larger than 100 per km^2. Indeed in these cases, less than 92% of the users are covered. In case popular contents are locally stored, the percentage of provisioned users becomes larger than 95% if 10% of the library is locally stored and it reaches 98% in case 25% of the library is cached on each UAV-BS.

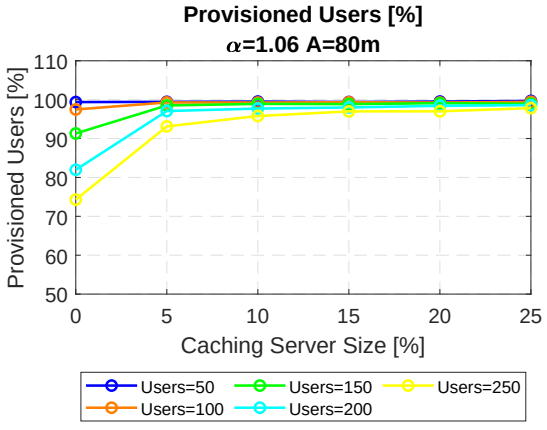

Figure 12: Provisioned Users (%) varying the number of users. A:Altitude.

6.6. Results Summary

A resume with the main results from our simulation of the flying caching server network with the three variations of the content popularity distribution and three capacities of the MEC server (0%, 10% and 25%) is recapped in Table 5. This is presented for the worst scenario of 250 $users/km^2$ and a flight height of 80 m. Notice that for a network without the MEC technology the values are the same for the three values of α. The user coverage rises to nearly 99% for a value of α equal to 1.56. The number of UAV-BS locations slightly increases from 11 to 12 drones when the capacity of the MEC server increases, particularly for values of α greater than one. The power consumption of the network only depends on the size of the MEC server and increments from 11.2 W per drone without caching technology to 42.2 W per drone for a 25% capacity. Despite this substantial variation, the variation of the flight time reduces only by 7.3 min from 76.9 min down to 69.6 min, requiring 6 drones per location for the whole 6 h of the event duration. The used capacity values are the ones with the major impact. Here we can see that the cache capacity could rise to 47.7 Mbps providing a total access capacity of 70.8 Mbps for α=1.56 and MEC server = 25%. Moreover, the backhaul capacity is reduced when the caching server is utilised from 41.8 Mbps down to 39.9, 32.2 and 23.1 Mbps for α= 0.56, 1.06 and 1.56 respectively. Finally, the delay values are improved from 497s to 458s, 398s and 329s for the different α values.

7. Conclusions and future work

The usage of fast deployable networks aided by UAV is considered the future of dynamic infrastructure, very useful to cope with the growth of the mobile traffic. However, several challenges arise from this technology such as optimal location and placement of drones under access, BH and power constraints in dynamic and crowed environments like concert festivals or sports matches. In these scenarios, where the attendants share a related interest, the chances that similar users download the same content is quite high.

In this paper we address this issue through the caching at the UAV-BS, provided by the MEC technology. We use a realistic network architecture, composed by a set of UAV-BSs, equipped with MEC servers that provide the caching capability. Results reveal that this is a very promising solution to avoid the BH network saturation, even if strictly dependant on the characteristics of the traffic, e.g. the popularity distribution of contents, and on the capacity of each MEC

server. We investigate the capacity of the MEC server (0% to 25%) and various content popularity distributions (Zipf distribution with α= 0.56, 1.06 and 1.56). To this end, we enhance a capacity simulation tool that is applied on a realistic scenario in the city centre of Ghent, Belgium, with realistic traffic acquired from an Italian mobile operator in the San Siro Stadium (Milan). Our simulation results show that the proposed architecture could increase the user coverage by 33% and access capacity by 70% while reducing the BH bandwidth usage down to 55% and decreasing the experienced delay by 33% with the implementation of the caching capabilities. Also, we prove that for highly popular content, a small server (5%) can provide more than 93% of requested traffic in the peak hour.

Future work will include realistic mobility behaviour from ground users, where handover and interference's analysis is included in addition to directional antennas on-board of the UAV-BS to deploy an optimal trajectory of the UAV-BS. The optimal solution of the network deployment could be addressed by using global functions or machine learning algorithms. In addition we want to overcome the unrealistic assumption of having a perfect knowledge of requested contents by implementing prediction algorithms, based on realistic data.

Acknowledgments

G. Castellanos was supported in part by the Colfuturo (Fundación para el futuro de Colombia), and in part by the Colombian School of Engineering - Julio Garavito, Doctoral scholarship Colfuturo-PCB 2018. M. Deruyck is a post-doctoral fellow of the FWO-V (Research Foundation – Flanders, ref.: 12Z5621N). Part of the work is founded by FWO project G098020N.

References

[1] F. Tariq, M. Khandaker, K.-K. Wong, M. Imran, M. Bennis, M. Debbah, A speculative study on 6g, arXiv preprint arXiv:1902.06700 (2019).

[2] T. Barnett, S. Jain, U. Andra, T. Khurana, Cisco visual networking index (VNI) (2022) 78.

[3] Y. Kawamoto, H. Nishiyama, N. Kato, F. Ono, R. Miura, Toward future unmanned aerial vehicle networks: Architecture, resource allocation and field experiments 26 (2019) 94–99.

[4] M. Mozaffari, W. Saad, M. Bennis, Y.-H. Nam, M. Debbah, A tutorial on UAVs for wireless networks: Applications, challenges, and open problems (2018).

[5] M. Deruyck, J. Wyckmans, W. Joseph, L. Martens, Designing UAV-aided emergency networks for large-scale disaster scenarios 2018 (2018).

[6] N. Zhao, W. Lu, M. Sheng, Y. Chen, J. Tang, F. R. Yu, K. Wong, UAV-assisted emergency networks in disasters 26 (2019) 45–51.

[7] B. Li, Z. Fei, Y. Zhang, UAV communications for 5g and beyond: Recent advances and future trends 6 (2019) 2241–2263. Conference Name: IEEE Internet of Things Journal.

[8] T. X. Tran, A. Hajisami, P. Pandey, D. Pompili, Collaborative mobile edge computing in 5g networks: New paradigms, scenarios, and challenges, IEEE Communications Magazine 55 (2017) 54–61.

[9] M. Chen, Y. Qian, Y. Hao, Y. Li, J. Song, Data-driven computing and caching in 5g networks: Architecture and delay analysis, IEEE Wireless Communications 25 (2018) 70–75.

[10] K. Poularakis, G. Iosifidis, L. Tassiulas, Approximation algorithms for mobile data caching in small cell networks, IEEE Transactions on Communications 62 (2014) 3665–3677.

[11] B. Blaszczyszyn, A. Giovanidis, Optimal geographic caching in cellular networks, in: 2015 IEEE international conference on communications (ICC), IEEE, pp. 3358–3363.

[12] X. Peng, J. Zhang, S. Song, K. B. Letaief, Cache size allocation in backhaul limited wireless networks, in: 2016 IEEE International Conference on Communications (ICC), IEEE, pp. 1–6.

[13] M. Mozaffari, W. Saad, M. Bennis, M. Debbah, Efficient deployment of multiple unmanned aerial vehicles for optimal wireless coverage 20 (2016) 1647–1650.

[14] A. Colpaert, E. Vinogradov, S. Pollin, Aerial coverage analysis of cellular systems at LTE and mmWave frequencies using 3d city models 18 (2018) 4311. Number: 12 Publisher: Multidisciplinary Digital Publishing Institute.

[15] S. De Bast, E. Vingradov, S. Pollin, Cellular coverage-aware path planning for UAVs (2019).

[16] A. V. Savkin, H. Huang, Deployment of unmanned aerial vehicle base stations for optimal quality of coverage 8 (2019) 321–324.

[17] G. Castellanos, M. Deruyck, L. Martens, W. Joseph, Performance evaluation of direct-link backhaul for UAV-aided emergency networks 19 (2019) 3342.

[18] G. Vallero, M. Deruyck, W. Joseph, M. Meo, Caching at the edge in high energy-efficient wireless access networks, in: ICC 2020-2020 IEEE International Conference on Communications (ICC), IEEE, pp. 1–7.

[19] G. Vallero, M. Deruyck, M. Meo, W. Joseph, Accounting for energy cost when designing energy-efficient wireless access networks, Energies 11 (2018) 617.

[20] E. Vinogradov, H. Sallouha, S. De Bast, M. M. Azari, S. Pollin, Tutorial on UAV: A blue sky view on wireless communication 14 (2018) 395–468.

[21] J. Wang, C. Jiang, Z. Han, Y. Ren, R. G. Maunder, L. Hanzo, Taking drones to the next level: Cooperative distributed unmanned-aerial-vehicular networks for small and mini drones, Ieee vehIcular technology magazIne 12 (2017) 73–82.

[22] A. A. Khuwaja, Y. Chen, N. Zhao, M.-S. Alouini, P. Dobbins, A survey of channel modeling for UAV communications 20 (2018). Conference Name: IEEE Communications Surveys Tutorials.

[23] R. Shakeri, M. A. Al-Garadi, A. Badawy, A. Mohamed, T. Khattab, A. K. Al-Ali, K. A. Harras, M. Guizani, Design challenges of multi-UAV systems in cyber-physical applications: A comprehensive survey and future directions 21 (2019) 3340–3385. Conference Name: IEEE Communications Surveys Tutorials.

[24] L. Gupta, R. Jain, G. Vaszkun, Survey of important issues in UAV communication networks 18 (2016) 1123–1152.

[25] M. Mozaffari, A. T. Z. Kasgari, W. Saad, M. Bennis, M. Debbah, Beyond 5g with UAVs: Foundations of a 3d wireless cellular network (2018).

[26] B. Alzahrani, O. S. Oubbati, A. Barnawi, M. Atiquzzaman, D. Alghazzawi, Uav assistance paradigm: State-of-the-art in applications and challenges, Journal of Network and Computer Applications 166 (2020) 102706.

[27] U. Challita, W. Saad, Network formation in the sky: Unmanned aerial vehicles for multi-hop wireless backhauling, in: GLOBECOM 2017 - 2017 IEEE Global Communications Conference, pp. 1–6.

[28] M. Gapeyenko, V. Petrov, D. Moltchanov, S. Andreev, N. Himayat, Y. Koucheryavy, Flexible and reliable uav-assisted backhaul operation in 5g mmwave cellular networks, IEEE Journal on Selected Areas in Communications 36 (2018) 2486–2496.

[29] B. Galkin, J. Kibilda, L. A. DaSilva, Backhaul for low-altitude uavs in urban environments, in: 2018 IEEE International Conference on Communications (ICC), pp. 1–6.

[30] A. Fouda, A. S. Ibrahim, I. Guvenc, M. Ghosh, Uav-based in-band integrated access and backhaul for 5g communications, in: 2018 IEEE 88th Vehicular Technology Conference (VTC-Fall), pp. 1–5.

[31] J. Pokorny, A. Ometov, P. Pascual, C. Baquero, P. Masek, A. Pyattaev,

A. Garcia, C. Castillo, S. Andreev, J. Hosek, Y. Koucheryavy, Concept design and performance evaluation of uav-based backhaul link with antenna steering, Journal of Communications and Networks 20 (2018) 473–483.

[32] M. Gerasimenko, J. Pokorny, T. Schneider, J. Sirjov, S. Andreev, J. Hosek, Prototyping directional uav-based wireless access and backhaul systems, in: 2019 IEEE Global Communications Conference (GLOBECOM), pp. 1–6.

[33] C. Qiu, Z. Wei, X. Yuan, Z. Feng, P. Zhang, Multiple uav-mounted base station placement and user association with joint fronthaul and backhaul optimization, IEEE Transactions on Communications (2020) 1–1.

[34] C. Qiu, Z. Wei, Z. Feng, P. Zhang, Backhaul-aware trajectory optimization of fixed-wing uav-mounted base station for continuous available wireless service, IEEE Access 8 (2020) 60940–60950.

[35] M. Youssef, J. Farah, C. Abdel Nour, C. Douillard, Full-duplex and backhaul-constrained uav-enabled networks using noma, IEEE Transactions on Vehicular Technology (2020) 1–1.

[36] M. M. U. Chowdhury, S. J. Maeng, E. Bulut, I. Güvenç, 3d trajectory optimization in uav-assisted cellular networks considering antenna radiation pattern and backhaul constraint, IEEE Transactions on Aerospace and Electronic Systems (2020) 1–1.

[37] K. Poularakis, G. Iosifidis, A. Argyriou, L. Tassiulas, Video delivery over heterogeneous cellular networks: Optimizing cost and performance, in: IEEE INFOCOM 2014-IEEE Conference on Computer Communications, IEEE, pp. 1078–1086.

[38] D. Liu, B. Chen, C. Yang, A. F. Molisch, Caching at the wireless edge: design aspects, challenges, and future directions, IEEE Communications Magazine 54 (2016) 22–28.

[39] B. Blaszczyszyn, A. Giovanidis, Optimal geographic caching in cellular networks, in: 2015 IEEE International Conference on Communications (ICC), pp. 3358–3363. ISSN: 1938-1883.

[40] M. Chen, Y. Hao, L. Hu, K. Huang, V. K. Lau, Green and mobility-aware caching in 5g networks, IEEE Transactions on Wireless Communications 16 (2017) 8347–8361.

[41] Z. Luo, M. LiWang, Z. Lin, L. Huang, X. Du, M. Guizani, Energy-efficient caching for mobile edge computing in 5g networks, Applied sciences 7 (2017) 557.

[42] K. Shanmugam, N. Golrezaei, A. G. Dimakis, A. F. Molisch, G. Caire, Femtocaching: Wireless content delivery through distributed caching helpers, IEEE Transactions on Information Theory 59 (2013) 8402–8413.

[43] N. Cheng, W. Xu, W. Shi, Y. Zhou, N. Lu, H. Zhou, X. Shen, Air-ground integrated mobile edge networks: Architecture, challenges, and opportunities 56 (2018) 26–32. Conference Name: IEEE Communications Magazine.

[44] M. Chen, M. Mozaffari, W. Saad, C. Yin, M. Debbah, C. S. Hong, Caching in the sky: Proactive deployment of cache-enabled unmanned aerial vehicles for optimized quality-of-experience 35 (2017) 1046–1061. Conference Name: IEEE Journal on Selected Areas in Communications.

[45] F. Liang, J. Zhang, B. Li, Z. Yang, Y. Wu, The optimal placement for caching uav-assisted mobile relay communication, in: 2019 IEEE 19th International Conference on Communication Technology (ICCT), pp. 540–544.

[46] N. Zhao, F. Cheng, F. R. Yu, J. Tang, Y. Chen, G. Gui, H. Sari, Caching UAV assisted secure transmission in hyper-dense networks based on interference alignment 66 (2018) 2281–2294. Conference Name: IEEE Transactions on Communications.

[47] H. Wang, G. Ding, F. Gao, J. Chen, J. Wang, L. Wang, Power control in UAV-supported ultra dense networks: Communications, caching, and energy transfer 56 (2018) 28–34. Conference Name: IEEE Communications Magazine.

[48] B. Jiang, J. Yang, H. Xu, H. Song, G. Zheng, Multimedia data throughput maximization in internet-of-things system based on optimization of cache-enabled UAV 6 (2019) 3525–3532. Conference Name: IEEE Internet of Things Journal.

[49] T. Li, K. Ota, T. Wang, X. Li, Z. Cai, A. Liu, Optimizing the coverage via the UAVs with lower costs for information-centric internet of things 7 (2019) 15292–15309. Conference Name: IEEE Access.

[50] X. Xu, Y. Zeng, Y. L. Guan, R. Zhang, Overcoming endurance issue: UAV-enabled communications with proactive caching 36 (2018) 1231–1244. Conference Name: IEEE Journal on Selected Areas in Communications.

[51] F. Zhou, N. Wang, G. Luo, L. Fan, W. Chen, Edge caching in multi-uav-enabled radio access networks: 3d modeling and spectral efficiency optimization, IEEE Transactions on Signal and Information Processing over Networks 6 (2020) 329–341.

[52] J. Ji, K. Zhu, D. Niyato, R. Wang, Joint cache placement, flight trajectory and transmission power optimization for multi-uav assisted wireless networks, IEEE Transactions on Wireless Communications (2020) 1–1.

[53] Y. Liu, S. Xie, Y. Zhang, Cooperative offloading and resource management for uav-enabled mobile edge computing in power iot system, IEEE Transactions on Vehicular Technology 69 (2020) 12229–12239.

[54] L. Yang, H. Yao, J. Wang, C. Jiang, A. Benslimane, Y. Liu, Multi-uav enabled load-balance mobile edge computing for iot networks, IEEE Internet of Things Journal (2020).

[55] S. Chai, V. K. N. Lau, Online trajectory and radio resource optimization of cache-enabled uav wireless networks with content and energy recharging, IEEE Transactions on Signal Processing 68 (2020) 1286–1299.

[56] M. Chen, W. Saad, C. Yin, Echo-liquid state deep learning for 360° content transmission and caching in wireless vr networks with cellular-connected uavs, IEEE Transactions on Communications 67 (2019) 6386–6400.

[57] Z. M. Fadlullah, N. Kato, Hcp: Heterogeneous computing platform for federated learning based collaborative content caching towards 6g networks, IEEE Transactions on Emerging Topics in Computing (2020) 1–1.

[58] M. Chen, W. Saad, C. Yin, Liquid state machine learning for resource and cache management in lte-u unmanned aerial vehicle (uav) networks, IEEE Transactions on Wireless Communications 18 (2019) 1504–1517.

[59] K. Shanmugam, N. Golrezaei, A. G. Dimakis, A. F. Molisch, G. Caire, Femtocaching: Wireless video content delivery through distributed caching helpers, arXiv preprint arXiv:1109.4179 (2011).

[60] J. Dai, Z. Hu, B. Li, J. Liu, B. Li, Collaborative hierarchical caching with dynamic request routing for massive content distribution, in: 2012 Proceedings IEEE INFOCOM, IEEE, pp. 2444–2452.

[61] N. Choi, K. Guan, D. C. Kilper, G. Atkinson, In-network caching effect on optimal energy consumption in content-centric networking, in: 2012 IEEE international conference on communications (ICC), IEEE, pp. 2889–2894.

[62] M. Deruyck, E. Tanghe, W. Joseph, W. Vereecken, M. Pickavet, B. Dhoedt, L. Martens, Towards a deployment tool for wireless access networks with minimal power consumption, in: 2010 IEEE 21st International Symposium on Personal, Indoor and Mobile Radio Communications Workshops, IEEE, 2010, pp. 295–300.

[63] A. A. per le Garanzie Nelle Comunicazioni, OSSERVATORIO SULLE COMUNICAZIONI N.4/ 2018, Technical Report N.4/2018, AGCOM - Autorita per le Garanzie Nelle Comunicazioni, 2018.

[64] W. Khawaja, I. Guvenc, D. Matolak, U.-C. Fiebig, N. Schneckenberger, A Survey of Air-to-Ground Propagation Channel Modeling for Unmanned Aerial Vehicles, arXiv:1801.01656 [eess] (2018). ArXiv: 1801.01656.

[65] A. Al-Hourani, S. Kandeepan, A. Jamalipour, Modeling air-to-ground path loss for low altitude platforms in urban environments, in: 2014 IEEE Global Communications Conference, pp. 2898–2904.

[66] 3GPP, 3GPP TR 36.777. 3rd Generation Partnership Project; Technical Specification Group Radio Access Network; Study on Enhanced LTE Support for Aerial Vehicles (Release 15), Technical Report, Valbonne - France, 2017.

[67] Microdornes, md4-1000: Robust and powerful – UAV / drone model from Microdrones, 2019.

[68] G. Castellanos, M. Deruyck, L. Martens, W. Joseph, System Assess-

ment of WUSN Using NB-IoT UAV-Aided Networks in Potato Crops, IEEE Access 8 (2020) 56823–56836. Conference Name: IEEE Access.

[69] ETSI, ETSI TS 136 212 v14.2.0 - LTE; Evolved Universal Terrestrial Radio Access (E-UTRA); Multiplexing and channel coding (3GPP TS 36.212 version 14.2.0 Release 14), Technical Report, ETSI, 2017.

[70] ETSI, ETSI TS 136 101 v14.5.0 - LTE; Evolved Universal Terrestrial Radio Access (E-UTRA); User Equipment (UE) radio transmission and reception (3GPP TS 36.101 version 14.5.0 Release 14), Technical Report, ETSI, 2017.

[71] ETSI, ETSI TS 136 213 v14.6.0 - LTE; Evolved Universal Terrestrial Radio Access (E-UTRA); Physical layer procedures (3GPP TS 36.213 version 14.6.0 Release 14), Technical Report, ETSI, 2018.

[72] H. Wu, Z. Han, K. Wolter, Y. Zhao, H. Ko, Deep learning driven wireless communications and mobile computing, 2019.

[73] K. Poularakis, G. Iosifidis, V. Sourlas, L. Tassiulas, Exploiting caching and multicast for 5g wireless networks, IEEE Transactions on Wireless Communications 15 (2016) 2995–3007.

[74] M. Deruyck, D. Renga, M. Meo, L. Martens, W. Joseph, Accounting for the varying supply of solar energy when designing wireless access networks, IEEE Transactions on Green Communications and Networking 2 (2017) 275–290.

[75] S. Sun, W. Jiang, G. Feng, S. Qin, Y. Yuan, Cooperative caching with content popularity prediction for mobile edge caching, Tehnički vjesnik 26 (2019) 503–509.

[76] E. E. Ugwuanyi, S. Ghosh, M. Iqbal, T. Dagiuklas, S. Mumtaz, A. Al-Dulaimi, Co-operative and hybrid replacement caching for multi-access mobile edge computing, in: 2019 European Conference on Networks and Communications (EuCNC), IEEE, pp. 394–399.

(BE'04, M'12) German Castellanos received a Bachelor degree in Electronics Engineering from the Colombian School of Engineering, Bogota, Colombia in 2004 and a specialization degree in Telematics and eBussines in 2006 from the same university. In 2012, he obtained a Master of Philosophy in Computer Engineering from the University of Newcastle, Australia. He is currently pursuing the Ph.D. degree in Electrical Engineering at Ghent University, Ghent, Belgium, with the IMEC – WAVES research group. From 2005, he has been a researcher with the ECITRONICA research group at the Colombian School of Engineering in Bogota, Colombia. Currently, he is an Assistant Professor from the Electronics Engineering program at the same university. His research interest includes new radio access network for mobile systems and coexistence between wireless services.

Greta Vallero got her bachelor degree in Computer Engineering, in Politecnico di Torino, in 2015; she then obtained the master degree with *summa cum laude*, in ICT for Smart Societies (Telecommunication Engineering), in October 2017, in Politecnico di Torino. From March 2017 to August 2017, she was hosted by Ghent University, in Belgium, to work on her master thesis, supervised by Prof. Michela Meo, in collaboration with Prof. Wout Joseph (Ghent University) and Dr. Margot Deruyck (Ghent University). In 2018, she starts officially her Ph.D., under the supervision of Professor Michela Meo, at Politecnico di Torino. Her main research interests are Multi-Access Edge Computing, as well as the energy efficiency in Radio Access Networks, using the support of Machine Learning algorithms, through radio resource management and network renewable energy supply.

Margot Deruyck was born in Kortrijk, Belgium, on July 14, 1985. She received the M. Sc. degree in Computer Science Engineering and the Ph. D. degree from Ghent University, Ghent, Belgium, in 2009 and 2015, respectively. From September 2009 to January 2015, she was a Research Assistant with Ghent University - IMEC – WAVES (Wireless, Acoustics, Environment & Expert Systems – Department of Information Technology). Her scientific work is focused on green wireless access networks with minimal power consumption and minimal exposure from human beings. This work led to the Ph.D. degree. Since January 2015, she has been a Postdoctoral Researcher at the same institution where she continues her work in green wireless access network.

Luc Martens received the M.Sc. degree in electrical engineering from Ghent University, Ghent, Belgium, in 1986, and the Ph.D. degree, in 1990. From 1986 to 1990, he was a Research Assistant with the Department of Information Technology, Ghent University. During this period, his scientific research focused on the physical aspects of hyperthermic cancer therapy. His research dealt with electromagnetic and thermal modelling, and the development of measurement systems for that application. Since 1991, he has been managing the WAVES Research Group, INTEC. The WAVES Research Group is part of the IMEC Institute, since 2004. Since 1993, he has been a Professor with Ghent University.

Michela Meo received the Laurea degree in electronic engineering and the Ph.D. degree in electronic and telecommunications engineering from the Politecnico di Torino, Italy, in 1993 and 1997, respectively, where she has been a Professor since 2006. She has co-authored about 200 papers and edited a book with Wiley and special issues of international journals, including ACM Monet, Performance Evaluation, and Computer Networks. Her research interests include performance evaluation and modelling, green networking, and traffic classification and characterization. She is an Associate Editor of the IEEE Communications Surveys & Tutorials and an Area Editor of the IEEE Transactions on Green Communications and Networking. He was an Associate Editor of the IEEE Transactions of Networking. She chairs the Steering Committee of IEEE OnlineGreenComm and the International Advisory Council of ITC. She was the Program Co-Chair of several conferences, including ACM MSWiM, IEEE GreenComm, IEEE ISCC, IEEE Infocom, and ITC.

(M'05) Wout Joseph was born in Ostend, Belgium on October 21, 1977. He received the M. Sc. degree in electrical engineering from Ghent University (Belgium) in July 2000. From September 2000 to March 2005, he was a research assistant at the Department of Information Technology (INTEC) of the same university. During this period, his scientific work was focused on electromagnetic exposure assessment. His research work dealt with measuring and modeling of electromagnetic fields around base stations for mobile communications related to the health effects of the exposure to electromagnetic radiation. This work led to a Ph. D. degree in March 2005. Since April 2005, he is postdoctoral researcher for IBBT-Ugent/INTEC (Interdisciplinary institute for BroadBand Technology). Since October 2007, he is a Post-Doctoral Fellow of the FWO-V (Research Foundation – Flanders). Since October 2009 he is professor in the domain of "Experimental Characterization of wireless communication systems." His professional interests are electromagnetic field exposure assessment, propagation for wireless communication systems, antennas and calibration. Furthermore, he specializes in wireless performance analysis and Quality of Experience.